1521-009X/12/4008-1538–1544$25.00
DRUG METABOLISM AND DISPOSITION
Vol. 40, No. 8
44008/3783651
DMD 40:1538–1544, 2012

Inhibition of P-Glycoprotein Leads to Improved Oral Bioavailability of Compound K, an Anticancer Metabolite of Red Ginseng Extract Produced by Gut Microflora[S]

Zhen Yang, Jing-Rong Wang, Tao Niu, Song Gao, Taijun Yin, Ming You, Zhi-Hong Jiang, and Ming Hu

Department of Pharmacological and Pharmaceutical Sciences, College of Pharmacy, University of Houston, Houston, Texas (Z.Y., T.N., S.G., T.Y., M.H.); Medical College of Wisconsin Cancer Center, Medical College of Wisconsin, Milwaukee, Wisconsin (M.Y.); and State Key Laboratory of Quality Research in Chinese Medicine, Macau Institute for Applied Research in Medicine and Health, Macau University of Science and Technology, Macau, China (J.-R.W., Z.-H.J.)

Received December 2, 2011; accepted May 10, 2012

ABSTRACT:

Ginsenosides are hydrolyzed extensively by gut microflora after oral administration, and their metabolites are pharmacologically active against lung cancer cells. In this study, we measured the metabolism of various ginsenosides by gut microflora and determined the mechanisms responsible for the observed pharmacokinetic behaviors of its active metabolite, Compound K (C-K). The results showed that biotransformation into C-K is the major metabolic pathway of ginsenosides after the oral administration of the red ginseng extract containing both protopanaxadiol and protopanaxatriol ginsenosides. Pharmacokinetic studies in normal mice showed that C-K exhibited low oral bioavailability. To define the mechanisms responsible for this low bioavailability, two P-glycoprotein (P-gp) inhibitors, verapamil and cyclosporine A, were used, and their presence substantially decreased C-K's efflux ratio in Caco-2 cells (from 26.6 to <3) and significantly increased intracellular concentrations (by as much as 40-fold). Similar results were obtained when transcellular transport of C-K was determined using multidrug resistance 1 (MDR1)-overexpressing Madin-Darby canine kidney II cells. In MDR1a/b(−/−) FVB mice, its plasma C_{max} and AUC_{0-24h} were increased substantially by 4.0- and 11.7-fold, respectively. These increases appear to be due to slower elimination and faster absorption of C-K in MDR1a/b(−/−) mice. In conclusion, C-K is the major active metabolite of ginsenosides after microflora hydrolysis of primary ginsenosides in the red ginseng extract, and inhibition/deficiency of P-gp can lead to large enhancement of its absorption and bioavailability.

Introduction

Ginsenosides, the dammarane-type triterpene saponins, have been found to be the major components responsible for ginseng's pharmacological activity, especially for the chemoprevention and inhibition of lung cancer. A major barrier to extending the clinical use of ginseng or ginsenosides is their low oral bioavailabilities, usually <5% in rodents (Xu et al., 2003; Qian et al., 2005; Joo et al., 2010). Low oral bioavailability may cause large variations in systemic exposure during clinical trials, which may lead to ambiguous results in the trials unless an extraordinarily large number of patients are enrolled. The latter is often too expensive to conduct. The low oral bioavailability of ginsenosides was attributed previously to their poor oral absorption, which is caused by a large molecular weight and bulky sugar moieties (Liu et al., 2009).

Compound K (C-K) (Fig. 1) is one of the extensively investigated ginsenosides that has displayed potent chemoprevention and anticancer activities in various cancer cell lines. Although C-K is of low abundance in raw ginseng or red ginseng extract, previous studies indicated that it could be the major metabolite after the oral administration of pure protopanaxadiol (PPD-type) ginsenosides (Akao et al., 1998a; Bae et al., 2000; Yoo et al., 2011). Earlier publications on ginsenoside metabolism by gut microflora usually used either pure 20-(*S*)-protopanaxadiol (PPD) or 20-(*S*)-protopanaxatriol (PPT) type ginsenosides (Akao et al., 1998a, 1998b; Tawab et al., 2003; Bae et al., 2005). However, the red ginseng extract containing both series (instead of individual ginsenosides) was usually the agent used for chemoprevention, because large quantities of purified ginsenosides are too costly for long-term use. Considering the complexity of ginseng extract, its metabolism profile may be different from that of single ginsenosides. Therefore, a better understanding of the metabolism of both PPD and PPT ginsenosides by gut microflora is necessary to monitor the disposition of ginsenoside by gut microflora.

This work was supported by the National Institutes of Health National Center for Complementary and Alternative Medicine [Grant AT005522] (to M.H. and M.Y.).

Article, publication date, and citation information can be found at http://dmd.aspetjournals.org.

http://dx.doi.org/10.1124/dmd.111.044008.

[S] The online version of this article (available at http://dmd.aspetjournals.org) contains supplemental material.

ABBREVIATIONS: C-K, Compound K; A, apical; B, basolateral; BCA, bicinchoninic acid; HBSS, Hanks' balanced salt solution; MDCKII, Madin-Darby canine kidney II; MDR1, multidrug resistance 1; MRT, mean residence time; MS, mass spectrometry; P-gp, P-glycoprotein; PPD, protopanaxadiol; PPT, protopanaxatriol; TOF, time-of-flight; UPLC, ultraperformance liquid chromatography.

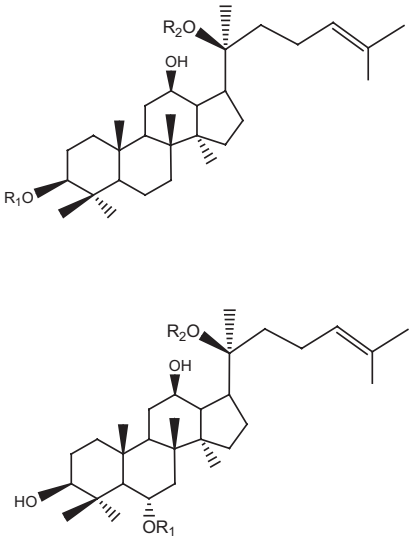

PPD series	R1	R2
Rb1	Glu^{2}-Glu	Glu^{6}-Glu
Rb2	Glu^{2}-Glu	Glu^{2}- Arap
Rc	Glu^{2}-Glu	Glu^{6}- Araf
Rd	Glu^{2}-Glu	Glu
F2	Glu	Glu
C-K	H	Glu
Rg3	Glu^{2}-Glu	H
Rh2	Glu	H

PPT series	R1	R2
Rh1	Glu	H
Rg1	Glu	Glu
Re	Glu^{2}-Rha	Glu
Rg2	Glu^{2}-Rha	H

FIG. 1. Chemical structures of ginsenosides of the PPD or PPT series. Glu, β-D-glucose; Arap, α-L-arabinose (pyranose); Araf, α-L-arabinose (furanose); Rha, α-L-rhamnose. These structures are shown here because their concentrations appear to have changed during the incubation of the red ginseng extract with microflora.

Despite the demonstration of the in vivo biotransformation of ginsenosides to C-K, C-K itself was reported to have low oral bioavailability (~5%) in rats (Lee et al., 2006; Paek et al., 2006). The absorption mechanism of C-K is generally considered to be passive diffusion, because one study showed that there was no difference between bidirectional transports in Caco-2 cells (Liu et al., 2009). However, there is evidence that C-K could reverse multidrug resistance in tumor cells (Hasegawa et al., 1994). In addition, our previous study on Rh2s, a ginsenoside analog with glucose attached to the C3 position and the same molecular weight and log *P* value as C-K, indicates that Rh2 underwent strong P-glycoprotein (P-gp)-mediated efflux both in vitro and in vivo (Yang et al., 2011).

P-gp is one of the most prevalent efflux transporters (Aller et al., 2009; Chen et al., 2011) and plays an important role in limiting the intestinal absorption of many compounds that are its substrates (Kusuhara and Sugiyama, 2002; del Amo et al., 2009). Inhibition of P-gp leads to the improvement of oral bioavailability of several anticancer drugs (Meerum Terwogt et al., 1998; Kemper et al., 2004; van Waterschoot et al., 2009), including ginsenoside Rh2 (Yang et al., 2011). A better understanding of P-gp involvement in the transport of ginsenosides and a more quantitative measurement with regard to if and how P-gp affects their bioavailabilities and potential drug-drug interactions are important for the development of ginsenosides as chemopreventive agents, because these studies are recommended by the Food and Drug Administration in recently published Drug-Drug Interaction Guidance (February, 2012, www.fda.gov).

In this study, we first investigated the metabolism of various ginsenosides present in a red ginseng extract in gut microflora and identified the major component after biotransformation by the microflora. We continued our efforts by determining the absorption mechanism of its major metabolite C-K to better understand the underlying mechanism responsible for its low oral bioavailability. Therefore, the aims of this study were as follows: 1) to delineate the dominant metabolism pathway of ginsenosides in gut bacteria lysate; and 2) to systemically investigate mechanisms responsible for the poor absorption of the active component, C-K, by elucidating which efflux transporter was mainly responsible for the efflux of C-K using a complementary set of in vitro and in vivo models.

Materials and Methods

Chemicals and Reagents. Ginsenosides Rb1 (purity >98%) was purchased from the National Institute for the Control of Pharmaceutical and Biological Products (Beijing, China); Rb2, Rc, Rd, 20-(*S*)-Rg3, 20-(*R*)-Rg3, 20-(*S*)-Rh2, and 20-(*R*)-Rh2 (each purity >98%) were purchased from Scholarbio-Tech (Chengdu, China). C-K and F2 (each purity >98%) were purchased from Must Bio-technology Co. Ltd. (Chengdu, China). Red ginseng extract was prepared by extracting red ginseng with water three times, and then the water extracts were concentrated and finally dried to powder (red ginseng extract) under low temperature. Rk1/Rg5 mixture (total purity >90%) was purified from processed red ginseng extract by silicon column chromatography and identified using high-resolution mass spectrometry (MS). All of the other chemicals were of analytical grade and used as received.

Cells. Cloned Caco-2 cells (TC7) were cultured as described previously (Hu et al., 1999). The lung carcinoma LM1 cell line was provided by Dr. Ming You's laboratory at the Medical College of Wisconsin. Parental Madin-Darby canine kidney II (MDCKII) and multidrug resistance 1 (MDR1)-MDCKII cells were provided by the Netherlands Cancer Institute (Amsterdam, The Netherlands). The inserts were purchased from Corning Life Sciences (Lowell, MA). Digoxin, cyclosporine A, verapamil, and Hanks' balanced salt solution (HBSS) (powder form) were purchased from Sigma-Aldrich (St. Louis, MO). Oral suspension vehicle was obtained from Professional Compounding Centers of America (Houston, TX). The bicinchoninic acid (BCA) protein assay kit was purchased from Thermo Fisher Scientific (Waltham, MA). All of the other materials (typically analytical grade or better) were used as received.

Animals. Male FVB and A/J mice (6–10 weeks of age) were purchased from Harlan (Indianapolis, IN). Male MDR1a/b knockout mice (6–10 weeks of age) were purchased from Taconic Farms (Germantown, NY). They were acclimated in an environmentally controlled room (temperature 25 ± 2°C, humidity 50 ± 5%, 12-h dark/light cycle) for at least 1 week before the experiments. The mice were fed with rodent diet (LabDiet 5001, www.labdiet.com) and fasted overnight before starting the pharmacokinetic studies.

Cell Culture. The Caco-2 cell culture has been maintained routinely in this laboratory over the last two decades (Hu and Borchardt, 1990, 1992). The culture conditions for growing Caco-2 cells were the same as those described previously (Yang et al., 2010). The transendothelial electrical resistance value >445 Ω/cm^2 was used as a quality control to test the tightness of the tight junction in Caco-2 cells. Parental MDCKII and MDR1-MDCKII cells were cultured in Dulbecco's modified Eagle's medium supplemented with 10% fetal bovine serum, 1% nonessential amino acids, 100 U/ml penicillin, and gentamicin. The expression levels of MDR1 in MDR1-MDCKII cells were monitored by Western blot analyses. LM1 is a metastatic cell line derived from A/J

mice (Zhang et al., 2003), which is the strain used for lung cancer carcinogenesis and chemoprevention studies (Yan et al., 2007). LM1 cells were grown in Dulbecco's modified Eagle's medium supplemented with 10% fetal bovine serum, 2 mM glutamine, 50 U/ml penicillin, 50 pg/ml streptomycin, and 1% nonessential amino acids. LM1 cells were seeded at 5×10^3 cells per well (96-well plate). LM1 cells were fed every day, and cells were ready for use 2 to 3 days after seeding.

Hydrolysis of Ginsenosides by Glycosidases Prepared from Mouse Gut Microflora. Fresh feces were collected using the A/J mice. One part of feces was mixed with 10 parts (volumes) of 0.1 mM ice-cold potassium phosphate buffer. They were vortexed for 30 s and sonicated in an ice-cold water bath for 30 min. The suspension was subjected to centrifugation at 1000 rpm and 4°C for 30 min. The final supernatant of the fecal homogenate was stored in aliquots at −80°C until use. Protein concentrations were determined by the BCA protein assay kit, using bovine serum albumin as the protein standard.

Frozen fecal homogenate was thawed, and 200 μl was added to the disposable glass vials. The homogenate was diluted with ice-cold potassium phosphate buffer to 2 ml. Red ginseng extract then was added to make the final concentration 1 mg/ml, and the study was performed in triplicate. The mixture was incubated at 37°C and shaken at 120 rpm for 24 h. Samples (100 μl) were taken at 0, 4, and 24 h, and the reaction was stopped with the addition of 500 μl of 2.5 μM testosterone (internal standard) in 100% acetonitrile. After centrifugation, 10 μl of the supernatant solution was injected into the quadrupole time-of-flight (TOF) mass spectrometer for analysis.

Transcellular Transport Study. The transcellular transport study was performed as described previously, and the permeabilities from the apical to basolateral side ($P_{a\text{-}b}$) and the basolateral to apical side ($P_{b\text{-}a}$) were calculated based on the method we described previously (Yang et al., 2011). In brief, 2.5 ml of C-K solution was loaded onto one side of the cell monolayer, and 2.5 ml of blank HBSS was loaded onto the other side. Five sequential samples (0.5 ml) were taken at different times (0, 1, 2, 3, and 4 h) from both sides of the cell monolayer. The same volumes of C-K solution and receiver medium (fresh HBSS) were added immediately to replace the volume lost as the result of sampling. The pH values of HBSS on both the apical and the basolateral sides were 7.4.

Intracellular concentrations of C-K were determined at the end of a transport study. The protocol for determining C-K's intracellular amounts in the cells was the same as that described previously (Yang et al., 2011). The protein concentration of the cell lysate was measured using the BCA protein assay kit.

Pharmacokinetic Studies of C-K in Wild-Type and MDR1a/b(−/−) FVB Mice. The animal protocols used in this study were approved by the University of Houston's Institutional Animal Care and Uses Committee. Pharmacokinetic studies of C-K were performed in wild-type and MDR1a/b(−/−) FVB mice to investigate the role of MDR1 or P-gp in limiting the bioavailability of C-K. C-K dispersed in the oral suspending vehicle was given by gavage to each group of mice at 10 mg/kg. The ingredients of the oral suspending vehicle are shown in Supplemental Table 1. Each pharmacokinetic study was performed using five mice, and 10 timed blood samples (20–25 μl) were taken by snipping their tails after the mice were anesthetized with isoflurane gas. The blood samples were collected in heparinized tubes and stored at −20°C until analysis.

Qualitative Determination of Microflora-Generated Secondary Ginsenosides. An ACQUITY ultra-performance liquid chromatography (UPLC) system (Waters, Milford, MA) coupled to a MicroTOF mass spectrometer (Bruker, Newark, DE) with an electrospray ionization source was used to qualitatively identify the metabolites of ginsenosides in gut microflora. Identification of ginsenosides and related metabolites was achieved by comparing

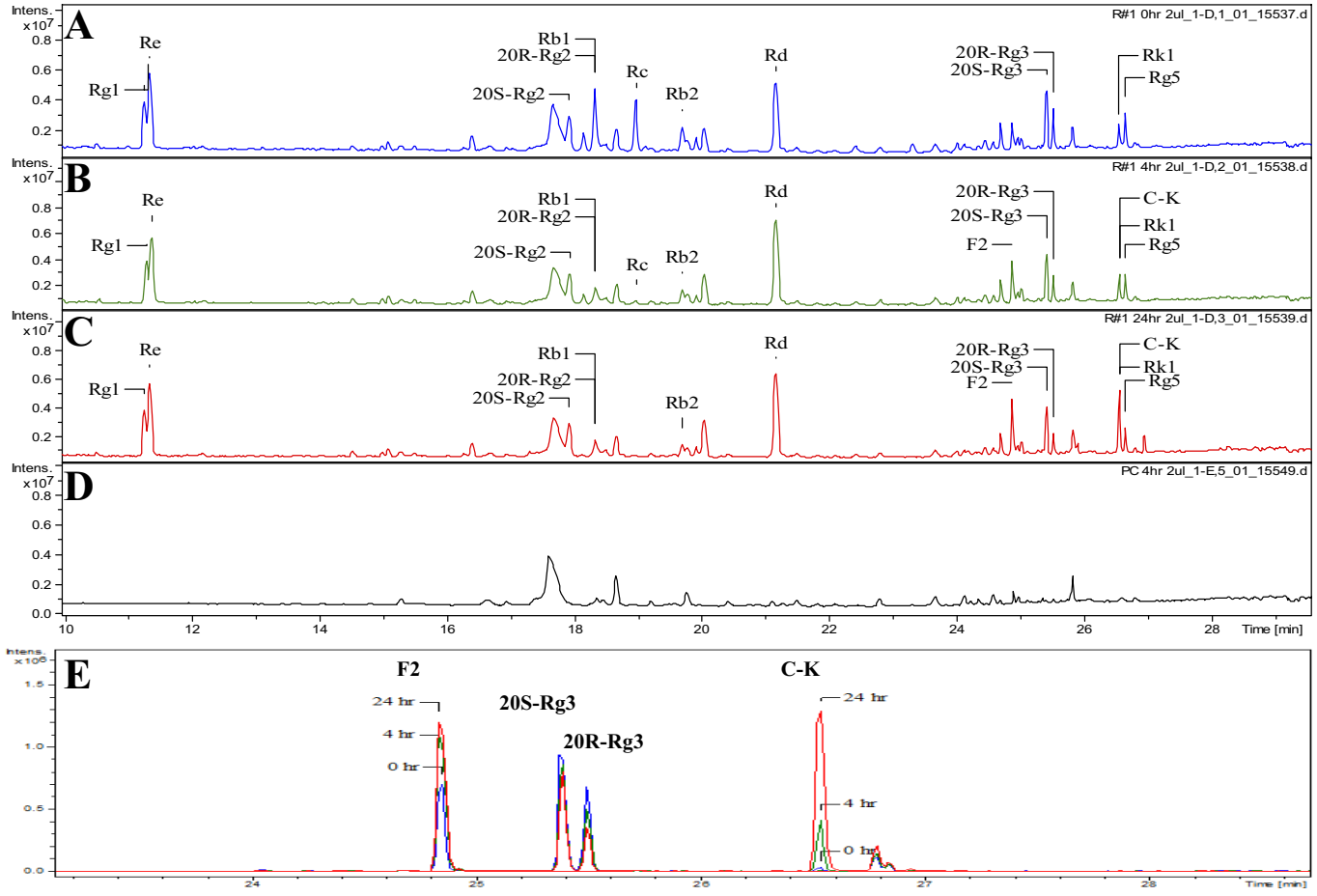

FIG. 2. UPLC-TOF-MS chromatograms of ginsenosides present in the red ginseng extract incubated in gut bacteria collected from A/J mice at 0 (A), 4 (B), and 24 h (C), blank fecal extraction without ginsenosides (4 h; D), and overlaid chromatograms of F2, C-K, Rg3r, and Rg3s at different time points where 0 h was marked as blue, 4 h was marked as green, and 24 h was marked as red (E) ($n = 3$).

the retention times with those of authentic compounds in combination with accurate mass. The chromatography and MS parameters are shown in Supplemental Table 2.

Quantitative Determination of C-K. An API 3200 Qtrap triple-quadrupole mass spectrometer (Applied Biosystems/MDS Sciex, Foster City, CA) equipped with a TurboIonspray source, operated in a positive ion mode, was used to quantitatively measure C-K in various matrices. The quantification was performed using multiple reaction monitoring mode with 645.0/203.0 (*m/z*) for C-K and 269.2/197.1 (*m/z*) for formononetin (internal standard). The other MS and UPLC parameters are shown in Supplemental Table 3.

The standard curves of C-K were linear in the concentration range from 19.5 nM to 10 μM, and the lower limit of quantitation was 9.8 nM in mouse blood. The intraday and interday precisions were within 15% for all of the quality control samples at three concentration levels (2.5, 0.3125, and 0.039 μM). A volume of 200 μl of methanol (containing 1 μM formononetin) was added to a 20-μl aliquot of a mouse blood sample. The supernatant was evaporated to dryness at 40°C under air and reconstituted in 100 μl of 100% methanol (v/v), and a 10-μl portion of each sample was injected into the UPLC-MS/MS system for analysis.

Pharmacokinetic Analysis. WinNonlin 3.3 (Pharsight Corporation, Mountain View, CA) was used for C-K and F2 pharmacokinetic analysis. The noncompartmental model was applied for the pharmacokinetic analysis of C-K profiles. Pharmacokinetic parameters, including C_{max}, T_{max}, k_e, half-life, mean residence time (MRT), and AUC, were derived directly from WinNonlin.

Statistical Analysis. The data in this article are presented as mean ± S.D., if not specified otherwise. Significant differences were assessed by using Student's *t* test or one-way analysis of variance. A *p* value of <0.05 was considered statistically significant.

Results

Hydrolysis of Ginsenoside by Glycosidases Derived from Gut Microflora Homogenate. After incubation with glycosidases prepared from gut microflora, the concentrations of Rb1, Rb2, and Rc in the red ginseng extract decreased with time (Fig. 2). Rc was hydrolyzed completely, whereas Rb1 and Rb2 were hydrolyzed >80% (estimated from peak area) at 24 h (Fig. 2, A and C). As a result, they were transformed into serial deglycosylated products, Rd, F2, and C-K. Both F2 and C-K kept increasing at 4 and 24 h compared with 0 h, whereas Rd did not show any obvious change in terms of peak area (Fig. 2, A–C), probably because it is the key intermediate of hydrolysis. Blank fecal extraction did not interfere with ginsenoside analytes in chromatography (Fig. 2D). In contrast, PPT-type ginsenosides (Re, Rg1, and Rg2) were not found to be metabolized during the 24-h incubation period (Fig. 3). To better visualize metabolites change with time, UPLC-TOF-MS chromatograms from different time points were overlaid (Fig. 1E), and F2 and C-K kept increasing, whereas both Rg3 and Rh2 decreased slightly with time (the peak of Rh2 was not shown). The likely metabolic scheme of PPD-type ginsenosides Rb1, Rb2, and Rc in the presence of PPT-type ginsenosides (as in the red ginseng extract) was proposed (Supplemental Fig. 1); however, it is noted that Rc may be converted to C-K via a different metabolic pathway (Shin et al., 2003; Yoo et al., 2011).

Transcellular Transport of C-K across Caco-2 Cell Monolayers. C-K was the major metabolite formed during the hydrolysis of red ginseng extract by mouse fecal homogenate. C-K has been shown to be active against multiple cancer cells (Chae et al., 2009; Kim et al., 2010; Wang et al., 2012), including against LM1 cells (Supplemental Fig. 2). Therefore, its absorption mechanisms were investigated further to better understand the reasons for its low oral bioavailability. The transcellular transport of digoxin was measured as the positive control before the C-K transport study was performed using Caco-2 cell monolayers. The results showed that the transcellular transport of

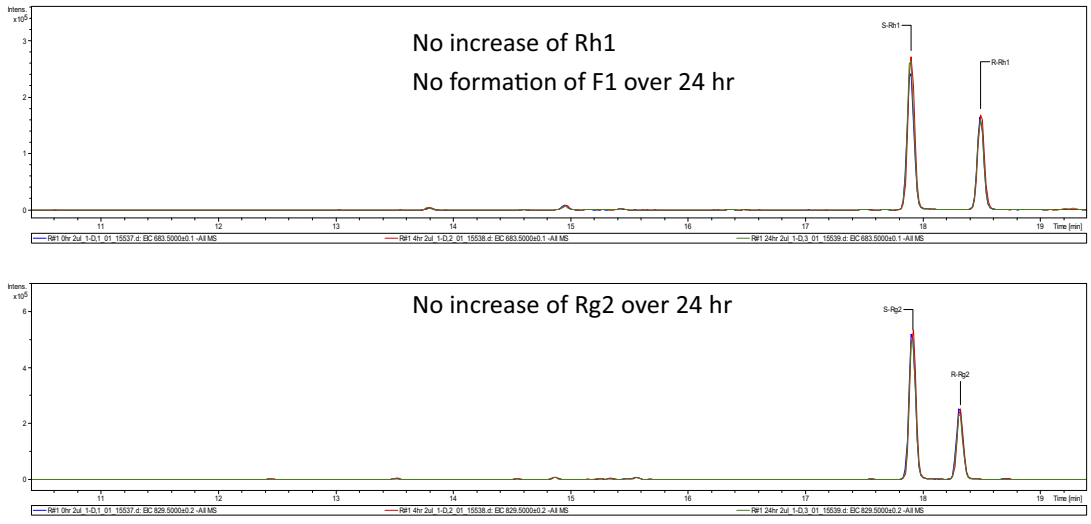

Compound	Peak Area		
	0hr	4hr	24hr
Rg1	4330743	4474314	4359311
Re	2810833	2787487	2760134
S-Rg2	2035730	2046414	2009334
R-Rg2	982891	983229	905223
S-Rh1	959337	1096862	1095979
R-Rh1	658923	647376	627316

FIG. 3. UPLC-TOF-MS chromatograms and peak areas of PPT-type secondary ginsenosides in the red ginseng extract incubated in gut bacteria collected from A/J mice at 0, 4, and 24 h. The top shows Rh1 and F1, and the bottom shows Rg2. The table underneath the chromatogram shows the peak areas of various compounds.

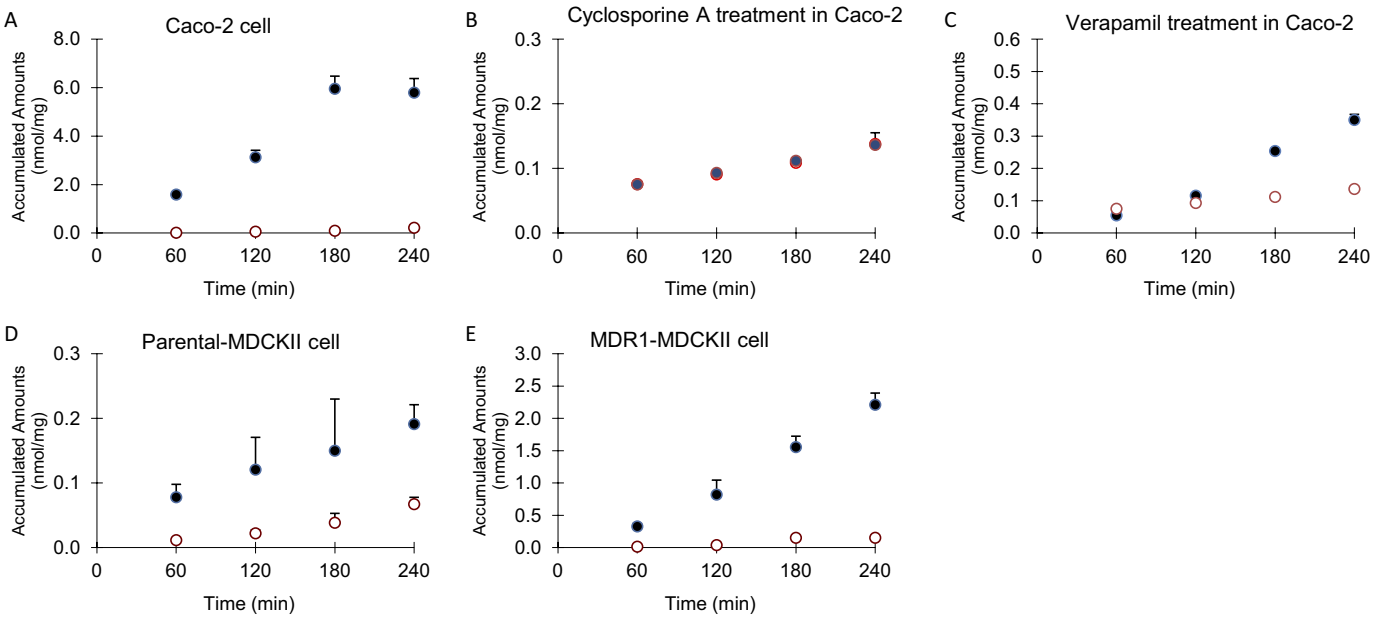

FIG. 4. Transcellular transport of 2 μM C-K across monolayers of Caco-2, parental MDCKII, and MDR1-MDCKII cells: A, C-K transport alone; B, C-K transport with 20 μM cyclosporine A; C, C-K transport with 50 μM verapamil; D, 2 μM C-K transport in parental MDCKII cells; E, 2 μM C-K transport in MDR1-MDCKII cells. Transport from A to B is represented by ○ and that from B to A is represented by ●. Data are presented as mean ± S.D. (n = 3).

digoxin displayed a significant efflux ratio (21.0), and $P_{a\text{-}b}$ was 1.48×10^{-6} cm/s, which was similar to our previous results (Yang et al., 2011). In the presence of 20 μM cyclosporine A, the efflux ratio of digoxin decreased from 21 to 1.2.

The results indicated that the transcellular transport of C-K (2 μM) across the Caco-2 monolayers from the basolateral (B)-to-apical (A) side (as measured by $P_{b\text{-}a}$) was significantly higher than the transport from the A-to-B side (Fig. 4A), and the efflux ratios ($P_{b\text{-}a}/P_{a\text{-}b}$) were 26.6 (Table 1). Two P-gp inhibitors, 50 μM verapamil or 20 μM cyclosporine A added to the apical side, were able to greatly inhibit the efflux transport of C-K (Fig. 4, B and C), and the efflux ratios were decreased to 2.9 (for verapamil) and 1.1 (for cyclosporine A), respectively. In the presence of inhibitors, $P_{a\text{-}b}$ was increased significantly by 2.9- and 2.8-fold, and $P_{b\text{-}a}$ was decreased significantly by 3.1- and 8.5-fold after verapamil and cyclosporine A treatment, respectively (Table 1). Consistent with the permeability results, two P-gp inhibitors also significantly increased the intracellular accumulation of C-K after treatment with 50 μM verapamil (from 0.01 to 0.50 nmol/mg) or 20 μM cyclosporine A (from 0.01 to 0.15 nmol/mg).

Transcellular Transport of C-K in MDR1-MDCKII Cells. Human MDR1/P-gp-overexpressing MDCKII cells were used to confirm the predominant role of P-gp in the transport of C-K. Before the transport studies of C-K, 2 μM digoxin was used as a positive control in the MDR1-MDCKII cell transport study. The efflux ratio of digoxin was 64.0 in MDR1-MDCKII cells, and $P_{a\text{-}b}$ is 2.98×10^{-7} cm/s, showing the normal expression of P-gp in MDR1-MDCKII cells.

The transport of C-K in parental MDCKII cells was used as a negative control, because they have low expression of human P-gp. As expected, the efflux ratio of C-K was much lower in parental MDCKII cells (Fig. 4D) compared with that in MDR1-MDCKII cells (Fig. 4E) at 2 μM (1.8 versus 18.2). However, $P_{a\text{-}b}$ of C-K was unexpectedly higher in MDR1-MDCKII cells (1.84×10^{-6} cm/s) than that of parental MDCKII cells (0.58×10^{-6} cm/s), which may be due to more effective tight junctions of MDCKII cell monolayers. The recoveries of C-K were within 85 to 115% in Caco-2 cells and both variants of MDCKII cells. The transport data also indicated a possible delay for transcellular transport, which is not uncommon and was reported in a previous publication (Hu et al., 1994). The intracellular accumulations of C-K also were measured, and the results showed that C-K accumulation was significantly higher (3.1-fold) in parental MDCKII cells (0.27 nmol/mg) than that in MDR1-MDCKII cells (0.08 nmol/mg; Table 1).

Effects of MDR1a/b Deletion on the Oral Bioavailabilities of C-K. To investigate whether MDR1/P-gp has major effects on the oral bioavailability of C-K, plasma profiles of C-K were compared between MDR1a/b (−/−) and wild-type FVB mice after oral dosing of

TABLE 1

Transcellular transport of C-K across monolayers of Caco-2, MDCKII, and MDR1-MDCKII cells in the absence or presence of P-gp inhibitors

Data are presented as mean ± S.D. (n = 3). $P_{a\text{-}b}$ refers to the permeability from the apical to basolateral side, and $P_{b\text{-}a}$ refers to the permeability from the basolateral to apical side. The values of permeability were compared between different directions, and intracellular amounts were compared to the control group. Data are the means ± S.D. of three independent experiments.

Cell Model	Inhibitor	Inhibitor Concentration	$P_{a\text{-}b}$	$P_{b\text{-}a}$	Efflux Ratio ($P_{b\text{-}a}/P_{a\text{-}b}$)	Intracellular Amounts
		μM	*×10⁻⁶ cm/s*	*×10⁻⁶ cm/s*		*nmol/mg*
Caco-2	–	–	1.16 ± 0.33	30.96 ± 4.31**	26.6	0.01 ± 0
	Verapamil	50	3.39 ± 0.41	9.89 ± 0.11*	2.9	0.50 ± 0.01***
	Cyclosporine A	20	3.30 ± 0.67	3.62 ± 0.22	1.1	0.15 ± 0.01***
MDCKII	–	–	0.58 ± 0.12	1.13 ± 0.11*	1.8	0.27 ± 0.03
MDR1-MDCKII	–	–	1.84 ± 0.70	33.64 ± 8.08**	18.2	0.08 ± 0.01**

–, indicated no inhibitor.
*, $P < 0.05$; **, $P < 0.01$; ***, $P < 0.001$.

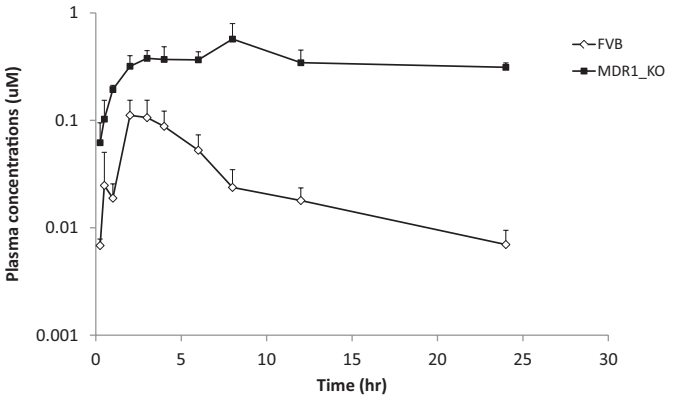

FIG. 5. The plasma concentrations of C-K in wild-type and MDR1a/b(−/−) FVB mice after the oral administration of C-K at 10 mg/kg. Data are presented as mean ± S.D. (n = 5).

C-K (10 mg/kg) (Fig. 5). A previous study showed that C-K exhibited linear pharmacokinetics in terms of AUC, clearance, and volume of distribution from 3 to 30 mg/kg (Lee et al., 2006); accordingly, the current dose (10 mg/kg) is appropriate to reveal the role of P-gp in the pharmacokinetics of C-K. In MDR1a/b(−/−) mice (on a FVB background), T_{max} was prolonged significantly (from 2.8 ± 0.84 to 5.6 ± 2.19 h, $p < 0.05$) compared with that of wild-type FVB mice. More importantly, plasma C_{max} was increased significantly by 4.0-fold ($p < 0.05$), and $AUC_{0\text{-}t}$ and $AUC_{0\text{-}\infty}$ were increased significantly ($p < 0.001$) by 11.7- and 23.5-fold, respectively, compared with those of wild-type FVB mice (Table 2).

In MDR1a/b(−/−) mice, k_e was decreased significantly (by 73%, from 0.13 ± 0.07 to 0.04 ± 0.01 h^{-1}, $p < 0.05$) compared with that of wild-type FVB mice. As expected, $t_{1/2}$ of C-K was increased significantly (by 3.2-fold, from 5.87 ± 3.04 to 18.68 ± 6.84 h, $p < 0.05$). Consistently, MRT also was increased significantly from 7.8 h (wild-type) to 30.8 h (knockout mice).

Discussion

This comprehensive study demonstrates unequivocally that C-K is a solid substrate of P-gp and that P-gp mediates the efflux of C-K in vitro and in vivo. Our results suggest that the inhibition of P-gp may represent a good strategy to improve the bioavailability of C-K. Because C-K is an active ginsenoside generated by intestinal microflora, its bioavailability may serve as a major indicator of in vivo bioavailability of PPD-type ginsenosides present in the red ginseng extract.

Our conclusion contradicts a previously published report that suggests passive diffusion as the major absorption mechanism for C-K, which was based on comparable bidirectional permeability values in the Caco-2 cell culture model (Liu et al., 2009). The discrepancy may due to the high substrate concentration (as much as 50 μM) they used, which may not be soluble or could have saturated the efflux process. Another major difference between the two studies is that we used Caco-2 TC7 (cloned) cells, whereas Liu et al. (2009) used wild-type Caco-2 cells. Published data indicated similar expression levels of P-gp in these two cell lines (Raeissi et al., 1999; Engman et al., 2001). Thus, we are not certain as to why there is this discrepancy, but our earlier article showed that our permeability results using Rh2 (Yang et al., 2011) also did not match their results using Rh2 (Liu et al., 2009). Our in vitro results obtained using chemical inhibitors of P-gp and the MDR1-overexpressing cell line support the conclusion that P-gp is the predominant efflux transporter responsible for C-K's in vitro disposition. These in vitro results are also consistent with our studies using P-gp knockout mice.

Our study using P-gp knockout mice suggests that in vivo bioavailability of C-K can be increased by inhibiting P-gp, because plasma AUC_{0-24h} of C-K was 12-fold higher in P-gp knockout mice than that in wild-type mice. Considering the oral bioavailability of C-K is reported to be ~5% in rodents (Lee et al., 2006; Paek et al., 2006), the current study demonstrated that the inhibition of P-gp should lead to significantly increased oral bioavailability of C-K. Our previous publication showed that the bioavailability of Rh2s, another active ginsenoside with a similar structure and also a solid substrate of P-gp, was increased from 1 to >30% by coadministering cyclosporine A in mice (Yang et al., 2011).

The mechanisms responsible for increased bioavailability of C-K in P-gp knockout mice appear to be decreased k_e and increased $t_{1/2}$ compared with those of wild-type mice (Table 2) and increased absorption (Table 1). The trend of slow elimination in MDR1a/b(−/−) mice was very obvious, although our last sample time was not long enough (<2 times $t_{1/2}$) to determine k_e and $t_{1/2}$ with high accuracy (Fig. 5). Considering the results of the transport studies using Caco-2 and MDR1-MDCK cell monolayers, increased absorption of C-K likely contributed to the increased plasma C_{max} and oral bioavailability of C-K in MDR1a/b(−/−) mice. Moreover, the slower elimination and longer half-life may be attributed to less biliary excretion during the terminal phase, assuming that the absorption phase would end sooner in P-gp knockout mice because of faster absorption of the same dose. Taken together, P-gp-mediated efflux appears to be responsible for C-K's low bioavailabilities, and in absence of this efflux mechanism, C-K would have a much higher oral bioavailability. This conclusion differs significantly from the previous observation that passive diffusion is the major absorption mechanism for this ginsenoside (C-K) (Liu et al., 2009).

Our results showed that PPD-type ginsenosides (Rb1, Rb2, and Rc) were metabolized extensively, whereas PPT-type ginsenosides (Rg1 and Re) were not metabolized significantly by glycosidases derived from the intestinal microflora of A/J mice. Two pieces of evidence demonstrate that Rg1 and Re were not metabolized. First, the peak area of Rg1 and Re stayed unchanged from 0 to 24 h. Second, if Rg1 and Re were metabolized, then we should have observed the formation of their metabolites, Rg2, Rh1, and/or F1, but none of these metabolites was found (Fig. 3). Our findings are different from those of previous reports on the metabolism of PPT-type ginsenosides by human intestinal microflora. Tawab et al. (2003) showed that Rg1 and

TABLE 2

The pharmacokinetic parameters of C-K (10 mg/kg) in FVB and MDR1a/b(−/−) FVB mice after oral administration

Data are presented as mean ± S.D. (n = 5).

Animal Strain	T_{max}	C_{max}	k_e	$t_{1/2}$	MRT_{inf}	$AUC_{0\text{-}t}$	$AUC_{0\text{-}\infty}$
	h	μM	h^{-1}	h	h	$h \cdot \mu M$	$h \cdot \mu M$
Wild-type FVB	2.8 ± 0.84	0.13 ± 0.03	0.13 ± 0.07	5.87 ± 3.04	7.82 ± 1.73	0.66 ± 0.19	0.75 ± 0.21
MDR1a/b(−/−) FVB	5.6 ± 2.19*	0.53 ± 0.23*	0.04 ± 0.01†,*	18.68 ± 6.84†,*	30.72 ± 8.62†,*	7.70 ± 2.27***	17.58 ± 16†,***

*, $P < 0.05$; **, $P < 0.01$; ***, $P < 0.001$.

† Estimated pharmacokinetic parameters may not be very accurate due to limited sample time (24 h) in MDR1a/b(−/−) mice.

Re could be metabolized extensively in human intestine by microflora, and Bae et al. (2005) showed that human fecal specimens could metabolize Re via stepwise deglycosylation to Rg1, F1, and aglycone. These results suggested that in A/J mouse microflora the metabolism of PPD-type ginsenosides is the predominant metabolic pathway compared with PPT-type ginsenosides when both of them were present (as in the red ginseng extract). The plasma profile of C-K after the oral administration of red ginseng extract at 200 mg/kg in A/J mice further confirmed the conversion of primary PPD-type ginsenosides into C-K by gut microflora in vivo (Supplemental Fig. 2).

C-K showed significant anticancer activity with $IC_{50} = 18.45$ μM, whereas F2 and the red ginseng extract did not show a significant antiproliferative effect in LM1 cells (Supplemental Fig. 3). Likewise, ginsenosides with the number of sugars greater than that of F2, including Rb1, Rb2, Rd, and Rc, also had lower activities (against LM1 cells) than F2 (Z. Yang and M. Hu, unpublished observations). The results were consistent with several structure-activity relationship studies, which showed that the anticancer activity of ginsenoside is correlated inversely to the number of sugars, which means the deglycosylation products have stronger anticancer activities than the precursor ginsenosides (Li et al., 2009; Musende et al., 2009). Because intestinal microflora are mainly responsible for this deglycosylation reaction, gut bacteria play an important role in ginsenoside effects in vivo.

In summary, we demonstrated clearly that C-K is the major metabolite of primary PPD-type ginsenosides in the red ginseng extract after they were hydrolyzed by glycosidases present in the gut microflora. C-K has low but significant oral bioavailability and displayed high in vitro inhibitory effects against lung cancer cells. Taken together, these findings may explain why ginsenosides such as C-K are active in vivo after the oral administration of the red ginseng extract that contains large quantities of primary ginsenosides that are inactive. Because C-K is a good substrate of P-gp and its absorption was greatly impeded by P-gp efflux, the inhibition of P-gp via increased absorption and/or decreased elimination may offer a viable strategy to significantly increase its oral bioavailability in vivo.

Acknowledgments

The pharmacokinetic data analysis was assisted by Dr. Diana Chow in College of Pharmacy, University of Houston.

Authorship Contributions

Participated in research design: Yang, You, and Hu.

Conducted experiments: Yang, Wang, Niu, Gao, and Yin.

Contributed new reagents or analytic tools: You and Jiang.

Performed data analysis: Yang, Wang, and Hu.

Wrote or contributed to the writing of the manuscript: Yang, Wang, Niu, and Hu.

References

Akao T, Kanaoka M, and Kobashi K (1998a) Appearance of compound K, a major metabolite of ginsenoside Rb1 by intestinal bacteria, in rat plasma after oral administration–measurement of compound K by enzyme immunoassay. *Biol Pharm Bull* **21:**245–249.

Akao T, Kida H, Kanaoka M, Hattori M, and Kobashi K (1998b) Intestinal bacterial hydrolysis is required for the appearance of compound K in rat plasma after oral administration of ginsenoside Rb1 from Panax ginseng. *J Pharm Pharmacol* **50:**1155–1160.

Aller SG, Yu J, Ward A, Weng Y, Chittaboina S, Zhuo R, Harrell PM, Trinh YT, Zhang Q, Urbatsch IL, et al. (2009) Structure of P-glycoprotein reveals a molecular basis for poly-specific drug binding. *Science* **323:**1718–1722.

Bae EA, Park SY, and Kim DH (2000) Constitutive beta-glucosidases hydrolyzing ginsenoside Rb1 and Rb2 from human intestinal bacteria. *Biol Pharm Bull* **23:**1481–1485.

Bae EA, Shin JE, and Kim DH (2005) Metabolism of ginsenoside Re by human intestinal microflora and its estrogenic effect. *Biol Pharm Bull* **28:**1903–1908.

Chae S, Kang KA, Chang WY, Kim MJ, Lee SJ, Lee YS, Kim HS, Kim DH, and Hyun JW (2009) Effect of compound K, a metabolite of ginseng saponin, combined with gamma-ray radiation in human lung cancer cells in vitro and in vivo. *J Agric Food Chem* **57:**5777–5782.

Chen L, Li Y, Zhao Q, Peng H, and Hou T (2011) ADME evaluation in drug discovery. 10. Predictions of P-glycoprotein inhibitors using recursive partitioning and naive Bayesian classification techniques. *Mol Pharm* **8:**889–900.

del Amo EM, Heikkinen AT, and Mönkkönen J (2009) In vitro-in vivo correlation in P-glycoprotein mediated transport in intestinal absorption. *Eur J Pharm Sci* **36:**200–211.

Engman HA, Lennernäs H, Taipalensuu J, Otter C, Leidvik B, and Artursson P (2001) CYP3A4, CYP3A5, and MDR1 in human small and large intestinal cell lines suitable for drug transport studies. *J Pharm Sci* **90:**1736–1751.

Hasegawa H, Matsumiya S, Murakami C, Kurokawa T, Kasai R, Ishibashi S, and Yamasaki K (1994) Interactions of ginseng extract, ginseng separated fractions, and some triterpenoid saponins with glucose transporters in sheep erythrocytes. *Planta Med* **60:**153–157.

Hu M and Borchardt RT (1990) Mechanism of L-alpha-methyldopa transport through a monolayer of polarized human intestinal epithelial cells (Caco-2). *Pharm Res* **7:**1313–1319.

Hu M and Borchardt RT (1992) Transport of a large neutral amino acid in a human intestinal epithelial cell line (Caco-2): uptake and efflux of phenylalanine. *Biochim Biophys Acta* **1135:**233–244.

Hu M, Chen J, Tran D, Zhu Y, and Leonardo G (1994) The Caco-2 cell monolayers as an intestinal metabolism model: metabolism of dipeptide Phe-Pro. *J Drug Target* **2:**79–89.

Hu M, Li Y, Davitt CM, Huang SM, Thummel K, Penman BW, and Crespi CL (1999) Transport and metabolic characterization of Caco-2 cells expressing CYP3A4 and CYP3A4 plus oxidoreductase. *Pharm Res* **16:**1352–1359.

Joo KM, Lee JH, Jeon HY, Park CW, Hong DK, Jeong HJ, Lee SJ, Lee SY, and Lim KM (2010) Pharmacokinetic study of ginsenoside Re with pure ginsenoside Re and ginseng berry extracts in mouse using ultra performance liquid chromatography/mass spectrometric method. *J Pharm Biomed Anal* **51:**278–283.

Kemper EM, Cleypool C, Boogerd W, Beijnen JH, and van Tellingen O (2004) The influence of the P-glycoprotein inhibitor zosuquidar trihydrochloride (LY335979) on the brain penetration of paclitaxel in mice. *Cancer Chemother Pharmacol* **53:**173–178.

Kim AD, Kang KA, Zhang R, Lim CM, Kim HS, Kim DH, Jeon YJ, Lee CH, Park J, Chang WY, et al. (2010) Ginseng saponin metabolite induces apoptosis in MCF-7 breast cancer cells through the modulation of AMP-activated protein kinase. *Environ Toxicol Pharmacol* **30:**134–140.

Kusuhara H and Sugiyama Y (2002) Role of transporters in the tissue-selective distribution and elimination of drugs: transporters in the liver, small intestine, brain and kidney. *J Control Release* **78:**43–54.

Lee PS, Song TW, Sung JH, Moon DC, Song S, and Chung YB (2006) Pharmacokinetic characteristics and hepatic distribution of IH-901, a novel intestinal metabolite of ginseng saponin, in rats. *Planta Med* **72:**204–210.

Li W, Liu Y, Zhang JW, Ai CZ, Xiang N, Liu HX, and Yang L (2009) Anti-androgen-independent prostate cancer effects of ginsenoside metabolites in vitro: mechanism and possible structure-activity relationship investigation. *Arch Pharm Res* **32:**49–57.

Liu H, Yang J, Du F, Gao X, Ma X, Huang Y, Xu F, Niu W, Wang F, Mao Y, et al. (2009) Absorption and disposition of ginsenosides after oral administration of Panax notoginseng extract to rats. *Drug Metab Dispos* **37:**2290–2298.

Meerum Terwogt JM, Beijnen JH, ten Bokkel Huinink WW, Rosing H, and Schellens JH (1998) Co-administration of cyclosporin enables oral therapy with paclitaxel. *Lancet* **352:**285.

Musende AG, Eberding A, Wood C, Adomat H, Fazli L, Hurtado-Coll A, Jia W, Bally MB, and Guns ET (2009) Pre-clinical evaluation of Rh2 in PC-3 human xenograft model for prostate cancer in vivo: formulation, pharmacokinetics, biodistribution and efficacy. *Cancer Chemother Pharmacol* **64:**1085–1095.

Paek IB, Moon Y, Kim J, Ji HY, Kim SA, Sohn DH, Kim JB, and Lee HS (2006) Pharmacokinetics of a ginseng saponin metabolite compound K in rats. *Biopharm Drug Dispos* **27:**39–45.

Qian T, Cai Z, Wong RN, Mak NK, and Jiang ZH (2005) In vivo rat metabolism and pharmacokinetic studies of ginsenoside Rg3. *J Chromatogr B Analyt Technol Biomed Life Sci* **816:**223–232.

Raeissi SD, Hidalgo IJ, Segura-Aguilar J, and Artursson P (1999) Interplay between CYP3A-mediated metabolism and polarized efflux of terfenadine and its metabolites in intestinal epithelial Caco-2 (TC7) cell monolayers. *Pharm Res* **16:**625–632.

Shin HY, Park SY, Sung JH, and Kim DH (2003) Purification and characterization of alpha-L-arabinopyranosidase and alpha-L-arabinofuranosidase from Bifidobacterium breve K-110, a human intestinal anaerobic bacterium metabolizing ginsenoside Rb2 and Rc. *Appl Environ Microbiol* **69:**7116–7123.

Tawab MA, Bahr U, Karas M, Wurglics M, and Schubert-Zsilavecz M (2003) Degradation of ginsenosides in humans after oral administration. *Drug Metab Dispos* **31:**1065–1071.

van Waterschoot RA, Lagas JS, Wagenaar E, van der Kruijssen CM, van Herwaarden AE, Song JY, Rooswinkel RW, van Tellingen O, Rosing H, Beijnen JH, et al. (2009) Absence of both cytochrome P450 3A and P-glycoprotein dramatically increases docetaxel oral bioavailability and risk of intestinal toxicity. *Cancer Res* **69:**8996–9002.

Wang CZ, Du GJ, Zhang Z, Wen XD, Calway T, Zhen Z, Musch MW, Bissonnette M, Chang EB, and Yuan CS (2012) Ginsenoside compound K, not Rb1, possesses potential chemopreventive activities in human colorectal cancer. *Int J Oncol* **40:**1970–1976.

Xu QF, Fang XL, and Chen DF (2003) Pharmacokinetics and bioavailability of ginsenoside Rb1 and Rg1 from Panax notoginseng in rats. *J Ethnopharmacol* **84:**187–192.

Yan Y, Cook J, McQuillan J, Zhang G, Hitzman CJ, Wang Y, Wiedmann TS, and You M (2007) Chemopreventive effect of aerosolized polyphenon E on lung tumorigenesis in A/J mice. *Neoplasia* **9:**401–405.

Yang Z, Gao S, Wang J, Yin T, Teng Y, Wu B, You M, Jiang Z, and Hu M (2011) Enhancement of oral bioavailability of 20(S)-ginsenoside Rh2 through improved understanding of its absorption and efflux mechanisms. *Drug Metab Dispos* **39:**1866–1872.

Yang Z, Gao S, Yin T, Kulkarni KH, Teng Y, You M, and Hu M (2010) Biopharmaceutical and pharmacokinetic characterization of matrine as determined by a sensitive and robust UPLC-MS/MS method. *J Pharm Biomed Anal* **51:**1120–1127.

Yoo MH, Yeom SJ, Park CS, Lee KW, and Oh DK (2011) Production of aglycon protopanaxadiol via compound K by a thermostable β-glycosidase from Pyrococcus furiosus. *Appl Microbiol Biotechnol* **89:**1019–1028.

Zhang Z, Futamura M, Vikis HG, Wang M, Li J, Wang Y, Guan KL, and You M (2003) Positional cloning of the major quantitative trait locus underlying lung tumor susceptibility in mice. *Proc Natl Acad Sci USA* **100:**12642–12647.

Address correspondence to: Dr. Ming Hu, Department of Pharmacological and Pharmaceutical Sciences, College of Pharmacy, University of Houston, 1441 Moursund St., Houston, TX 77030. E-mail: mhu@uh.edu